Nature of the Metal–Support Interaction in Bifunctional Catalytic Pt/H-ZSM-5 Zeolite

ARTICLE *in* THE JOURNAL OF PHYSICAL CHEMISTRY B · JULY 2005

Impact Factor: 3.3 · DOI: 10.1021/jp0511348 · Source: PubMed

4 AUTHORS, INCLUDING:

Piti Treesukol
Kasetsart Univeristy, Thailand, Nakhonpathom
7 PUBLICATIONS **232** CITATIONS
SEE PROFILE

Kanokthip Boonyarattanakalin
King Mongkut's Institute of Technology Ladk…
3 PUBLICATIONS **69** CITATIONS
SEE PROFILE

Thanh Truong
University of Utah
169 PUBLICATIONS **6,239** CITATIONS
SEE PROFILE

Nature of the Metal−Support Interaction in Bifunctional Catalytic Pt/H-ZSM-5 Zeolite

Piti Treesukol,[†,§] Kanokthip Srisuk,[‡] Jumras Limtrakul,*[,‡] and Thanh N. Truong*[,†]

Henry Eyring Center for Theoretical Chemistry, University of Utah, Salt Lake City, Utah, 84112, Faculty of Liberal Arts and Science, Kasetsart University, Kampaeng Saen Campus, Nakornpathom, Thailand 70320, and Laboratory for Computation and Applied Chemistry, Kasetsart University, Bangkok, Thailand 10900.

Received: March 4, 2005; In Final Form: April 25, 2005

The metal−support interaction of a dispersed Pt atom on H-ZSM-5 zeolite has been investigated by using an embedded cluster and cluster models with the density functional theory/B3LYP functional method. We found that the Pt atom interacts with a Brønsted proton and a nearby framework oxygen. Interaction with the framework oxygen causes electron transfer from the zeolite to the Pt atom. Concurrently, a Brønsted proton stabilizes the Pt atom on the zeolite surface by withdrawing excess electron density from the Pt atom. These charge transfers result in a zero net charge on the Pt atom while changing its orbital occupation. The binding energy of Pt on the Brønsted acid was 15 kcal/mol. Inclusion of the Madelung potential by Surface Charge Representation of the Electrostatic Embedded Potential method (SCREEP) had small effects on structure and charge density of Pt/H-ZSM-5 but it shifted the stretching mode of CO toward a higher frequency by almost 40 cm^{-1}. The frequency shift of absorbed CO calculated with embedded cluster models was from 8 to 11 cm^{-1} red shift, compared to 20 cm^{-1} red shift from experiment. This implies that not only the electronic state of the Pt atom but also the Madelung potential of the support is responsible for the observed small red shift of CO on the Pt-H-ZSM-5.

1. Introduction

Supported platinum particles on oxide surfaces, such as SiO_2, Zr_2O_3, Ti_2O_3, or zeolite, have outstanding catalytic activity in many processes, e.g., (de)hydrogenation,[1,2] isomerization,[3] oxidation,[4−6] aromatization,[7,8] and automotive exhaust catalysis.[9] Basically, the main purpose of using support materials is to maintain the dispersion of metal particles, but experimental studies have revealed that the supports can also modify the catalytic properties of metal particles significantly. The catalytic reactivity of the supported metal can be tuned as desired if the metal−support interaction is well understood. Nevertheless, the nature of the metal−support interaction is still elusive.[10−14]

Transition metals supported on zeolite have been found to be active catalysts for many processes.[3,8,15−17] The performance and selectivity of the catalyzed processes depend on the nature of the metals and of the zeolite acidic sites. Much attention has been focused on the zeolite-supported platinum, which is a very active and very stable catalyst for hydrocracking, hydroisomerization, and reforming of hydrocarbons.[17−23] The acid site of zeolite is suggested, not only to alter the catalytic property of the metal cluster, but also to have a key role in the catalytic process. Two active centers of the Pt/H-ZSM-5 (the metal particle and the acid site) may work collaboratively as the bifunctional catalyst. A model to explain the mechanism of bifunctional catalysts has been proposed: the (de)hydrogenation and ring opening occur on the metal particle while the isomerization through the carbonium ion intermediates occurs on the acid site.[24−26] Nevertheless, there is no explanation for the synergistic effect of the metal cluster and acidic support that is observed in many hydroconversion reactions.

Particle size, location, and the electronic state of supported Pt and the metal/support interaction are important factors that can affect the catalytic activity of Pt/zeolite. Studies on the Pt/zeolite-catalyzed dehydrogenation reaction have shown that a small size of the platinum particle correlates with a high turnover frequency (TOF).[27] The size of Pt clusters can be controlled by the preparation conditions and the acidity of the support.[8,17,28−31] From the fact that high acidic zeolites favor smaller Pt clusters, the metal/acid-site interaction is believed to have an important role in stabilizing dispersed metals. The differences in catalytic properties between bulk platinum and diffused Pt particles and the confined space within the zeolite framework suggest that the active Pt species in acidic zeolite must be very small to fit inside the zeolite framework.[11,32,33] Pt clusters ranging from 25 atoms in size to monatomic species have been identified, depending on the acidity and cavity size of the zeolite.[28,32,34−39] The most stable sites for isolated Pt atoms in zeolite were determined to be in sodalite cages for faujasite zeolite and in side pockets for mordenite zeolite.[36,38,39] These species are inaccessible for most guest molecules. For H-ZSM-5, Pt clusters are localized in the main channels, which are catalytically active and easily accessible for guest molecules.[37]

One of the most controversial issues regarding zeolite supported Pt is how the zeolite framework affects the electronic property of supported platinum. Explanations have been deduced mainly based on the CO-adsorption studies, in which a small red shift of CO has been observed. Many suggested that Pt clusters are in electron-deficient states and that they give rise to the remarkable catalytic property observed.[31,38,40−42] Whether the apparent electron deficiency of Pt particles stems from intrinsic properties of the small metal particles is still debatable.[11,31,43] Electron transfer from the metal particle to the

* Address correspondence to these authors: T. N. Truong (e-mail: truong@chem.utah.edu) and J. Limtrakul (e-mail: fscijrl@ku.ac.th).
† University of Utah.
§ Faculty of Liberal Arts and Science, Kasetsart University.
‡ Laboratory for Computation and Applied Chemistry, Kasetsart University.

10.1021/jp0511348 CCC: $30.25
Published on Web 06/01/2005

Brønsted proton is a straightforward explanation for the electron-deficient states of Pt.[11,12,44,45] However, alternative explanations exist.[27,34,43,46,47] For instance, Miller et al.[43] reported that the valence band of Pt on LTL zeolites, with a different acidity, showed no sign of electron transfer between Pt particles and zeolite. The interaction between the metal and support leads to a shift in the energy of the metal valence orbitals, which can stabilize the bonding between Pt and the adsorbate.[48]

Only a small number of theoretical studies on the systems of Pt/zeolite have been reported to date. The main purpose of those works was to look for structures of the Pt particles inside zeolites and a possible explanation for the observed CO red shift. Structures of the active centers of monatomic Pt in H-Mordenite were investigated by molecular mechanics and density functional methods.[49,50] Yakolev et al. used DFT/LDA with small zeolite cluster models (2T and 4T) to investigate the adsorption of CO on a supported Pt atom in the side pocket of H-Mordenite assuming specific Pt-acidic proton configurations.[50] The red shift of adsorbed CO (40−80 cm^{-1}) was interpreted as a consequence of an electron-deficient state of the Pt atom. Grillo and de Agudelo studied the structure of Pt/H-Mor and its interactions with hydrocarbons by molecular mechanics and molecular dynamics.[49,51] However, questions such as how metal−support interaction affects the electronic structure and properties of the metal particles upon adsorption have not been addressed so far. Previous calculations on the systems of small molecules on Pt/supports show the sensitivity of the vibrational frequencies of adsorbates not only on the electronic property of the adsorption site, but also on the support environments.[52−54] In this case, the environmental effect can complicate the interpretation of the CO frequency shift and the frequency shift may not be used as direct evidence for the deficient states of Pt clusters.

In this study, our objective is to understand metal−support interaction and how it affects the electronic structures and properties of the metal particles upon adsorption. We employed the monatomic Pt on H-ZSM-5 zeolite as a model for simplicity in our theoretical efforts but it also corresponds with the high TOF case.[27] The effect of the extended framework was examined by using an embedded cluster model. The adsorption of CO was investigated to examine the nature of the electronic state of the supported Pt. Other factors that can affect the results, such as the Pt particle size and the location of the Brønsted acid site, will be discussed in the future.

2. Methodology

The three different-sized cluster models (3T, 5T, and 10T, where T is Si or Al atom) shown in Figure 1a−c were used to represent the active site of the H-ZSM-5 zeolite framework. These models were taken from the crystallographic structure of the ZSM-5 zeolite and were optimized at the DFT/B3LYP level of calculation.[55] The clusters were parts of the 10T ring at the intersection of the zigzag and main channels, which is the most accessible region for guest molecules. One proton was added to each of the clusters to counterbalance the negative charge upon Al substitution on the T12-site Si tetrahedral in the framework. The T12 site has been found to be among the most stable Brønsted acidic sites in H-ZSM-5 zeolite.[56−58] All clusters were terminated at the boundary by hydrogen atoms aligning along the broken Si−O bond direction at a distance of 1.47 Å. The Brønsted acid site (Si−O(H)−Al−O−Si) was optimized while the rest was fixed to mimic the framework constraints. A Pt atom was added to the optimized H-ZSM-5 models. The adsorbed Pt atom of $5d^96s^1$ electronic configuration and the active site of H-ZSM-5 were reoptimized.

Comparison between the 3T and 5T models was made to determine the effect of the size of the zeolite model. The effect of the extended framework of zeolite was examined by means of an embedded cluster model, in which the Madelung potential from the infinite lattice is accounted for by using a set of point charges. The 5T cluster was embedded in two sets of point charges derived from the Surface Charge Representation of the Electrostatic Embedding Potential (SCREEP) method.[55,59−61]

Structures of CO adsorbed on Pt/H-ZSM-5 were obtained by partial optimization where the active site and the adsorbate were relaxed. Only the adsorption with a C-bound configuration will be discussed here because it has been found to be much more stable than the one with O-bound. Vibrational modes of the carbonyl complexes were calculated and compared to experimental data. The effects of the cluster size on the binding energy and vibrational frequency of CO adsorption were determined by performing both bare cluster and embedded 10T cluster calculations where the optimized structures from the 5T cluster model were used while the remaining quantum atoms of the 10T cluster were fixed at the experimental ZSM-5 lattice positions. The embedded 10T cluster model is shown in Figure 1c. The wireframe structure and pink dots surrounding the 10T quantum cluster represent two different sets of point charges, i.e., explicit charges and surface charges, of the SCREEP embedded model.

All calculations were carried out at the DFT/B3LYP level of calculation, which is well-known for its consistency and reliability for zeolite systems. The relativistic effect was considered to be significant for the Pt atom and it was accounted for by the use of the Hay-Wadt $VDZ_{(n+1)}$ basis set with the effective core potential for the Pt atom.[62] The 6-31G(d,p) basis set was used for all other atoms, except for the terminating hydrogens and two silanol groups at two ends of the cluster that were treated with the 3-21G basis set. The basis set superposition error (BSSE) was accounted for by the counterpoise method[63,64] where the BSSE corrected binding energy is approximated by $E^{CP}_{binding} = E_{Super} + \sum_{i=1,n}(E_{m_f^i} - E_{m_f^{i*}}) - \sum_{i=1,n}E_{m_{opt}^i}$. In this equation, E_{Super} is the total energy of the adsorption complex. E_{m^i}'s represent the energies of the individual species with the subscripts "opt" and "f" denoting individually optimized monomers and the monomers frozen in their adsorption complex geometries, with the superscript "$*$" representing monomers calculated with ghost orbitals. Partial charges and population analysis were determined by Natural Atomic Orbital (NAO) and Natural Bond Orbital (NBO) methods.[65] All calculations were done with the Gaussian 03 program.[66]

3. Results and Discussion

3.1. Structure of the Pt-H-ZSM-5 Active Center. The optimized structures of the active center with 3T and 5T clusters are shown in Figure 1a,b. Selected parameters of Pt/HZSM-5 systems are tabulated in Table 1. In all cases the Pt atom was located next to a Brønsted proton of the zeolite. We found that the choice of cluster model to represent the active site of H-ZSM-5 is crucial. In particular, using small clusters such as $H_3SiO(H)AlH_3$[67] caused fictitious interaction between the Pt atom and terminating hydrogen atoms and predicted that the Pt atom would bind only to the Brønsted proton. With use of the larger 5T cluster model, the calculated $Pt-O_N$ distance of 2.07 (Pt atom and the nearest bridging oxygen) and $Pt-O_B$ distance of 2.86 Å (Pt atom and Brønsted oxygen) agreed very well with the XANES and EXAFS finding of 2.18 and 2.7−2.9 Å for supported Pt on LTL zeolite.[31,32,43,47] The negligible changes in SiO bonds surrounding the acid site demonstrated that the Pt atom perturbed the zeolite structure only locally.

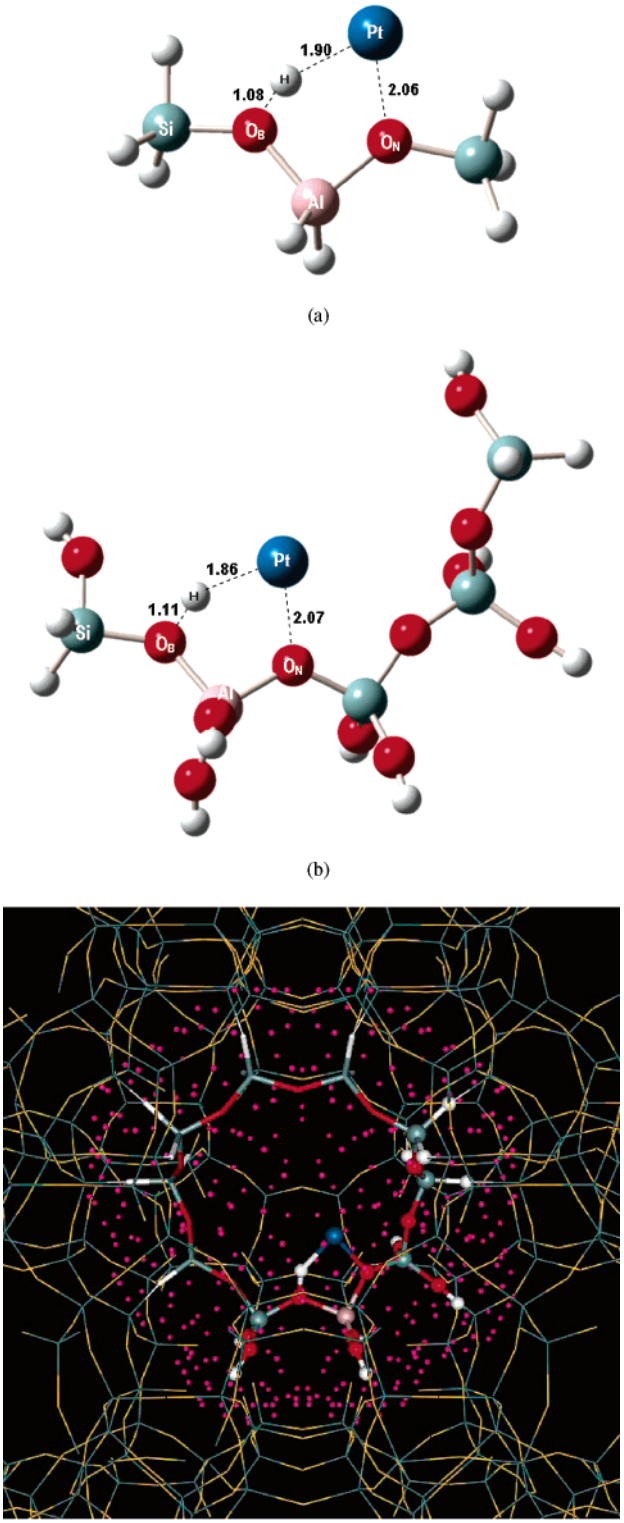

Figure 1. Optimized structures of monatomic Pt on H-ZSM-5 (a) 3T and (b) 5T cluster models (selected bond distances are in Å); (c) the embedded 10T cluster model where the structure of the ball and stick part is taken from the optimized 5T cluster model while the structure of the stick part is fixed to the experimental lattice positions.

It is interesting to note that without an acid site, the Pt atom bound very weakly on the zeolite surface (E_B < 1 kcal/mol). The BSSE corrected binding energies between Pt atom and H-ZSM-5 framework were predicted to be 18.9 and 15.0 kcal/mol from 3T and 5T cluster calculations, respectively. This result suggests that the Brønsted proton is necessary for binding a Pt atom to the zeolite framework and can be thought of as a nucleation center for Pt particles. However, the relatively small magnitude of the binding energy also suggests that at higher temperatures agglomeration of Pt atoms is possible. These results agree with experimental findings that large-size Pt clusters occur at high temperatures or in neutral or basic zeolite environments.[68−70]

NBO analysis shows bonding characteristics between the d-orbital of Pt and the Brønsted proton and between the sd-orbtial of Pt and the framework oxygen (Figure 2). The LUMO is an antibonding orbital between the Pt atom and framework oxygen. We also found that the interaction between supported Pt and the Brønsted proton creates a Pt−H antibonding orbital above the Fermi level of Pt/H-ZSM-5 as is also suggested by XANES studies.[27,34] The energy difference between the antibonding orbital and the Fermi level has been suggested to increase with increasing acidity of the support, correlating with the TOF for hydrogenolysis and isomerization processes.[27]

The charge densities calculated by Mulliken and by NAO population analysis display the same trend. The electronic configurations and partial charges calculated by NAO analysis are presented in Table 2. Our results show electron transfer between the Pt atom and the Brønsted acid site and the framework oxygen of H-ZSM-5 through bonding. An increase of electron density in s- and d-orbitals of Pt due to interaction with the framework oxygen and a decrease of electron density in other d-orbitals of Pt due to interaction with the Brønsted proton were observed from both Mulliken and NAO population analysis. The electron transfer from the framework oxygen strengthened the Pt−O_N bonding but the Pt atom was less stable in a negative oxidation state. The Brønsted proton can stabilize the Pt atom by withdrawing excess electron density from the Pt atom. This can explain why the aggregation of Pt atoms is likely for dispersed Pt on basic or neutral supports.

The 5T cluster model had more electron density localized at the acid site, consistent with a previous observation that a larger cluster can provide more electron density to the acid site.[55] The lower binding energy of Pt/H-ZSM-5 predicted by the 5T cluster model was probably due to more Coulombic repulsion between the Pt atom and the zeolite framework. The effect of an extended zeolitic framework on the structural and energetic properties of the active site of Pt/H-ZSM-5 has been examined. The effect of the Madelung potential on the active region of the Pt/H-ZSM-5 system was examined by using an SCREEP embedded cluster. We found that the external field from the extended framework has small effects on structure and charge density. The magnitudes of structural changes were on the order of hundredths of angstroms. The binding energy between Pt and zeolite was decreased by less than 1 kcal/mol. The differences are pronounced if the smaller cluster is employed.[55] This implies that the 5T cluster used in this study is sufficient to model the active site of Pt/H-ZSM-5.

3.2. Adsorption of CO. The configurations of CO adsorption on supported Pt systems are shown in Figure 3. Selected optimized parameters of CO adsorptions are reported in Tables 3 and 4. A previous DFT calculation utilized cluster models to represent a Pt atom stabilized in H-Mordenite by one or two Brønsted OH's and provided the Pt−C bond length of 1.76−1.77 Å, the Pt−H distance of 2.00 Å, and the adsorbed CO bond length of about 1.15−1.16 Å.[50] The authors also observed a linear CO adsorption on Pt atom with a C−Pt−H angle of 85°. The same adsorption configuration was found here. Carbon monoxide adsorbed linearly on the Pt atom (Pt−C−O ∼ 180°). The C−Pt−H angle was almost 90°, while the C−Pt−O_N angle

TABLE 1: Selected Optimized Geometrical Parameters (Å) and Binding Energies E_B (kcal/mol) of Pt/Support Systems[a]

systems	E_B[b]	R(SiO_B)	R(AlO_B)	R(O_BH)	R(AlO_N)	R(SiO_N)	*R*(Pt···H)	*R*(Pt···O_N)
HZ3		1.694	1.880	0.970	1.706	1.628		
PtHZ3	18.89	1.673	1.804	1.078	1.783	1.676	1.890	2.062
HZ5		1.704	1.850	0.971	1.681	1.599		
PtHZ5	15.00	1.677	1.776	1.108	1.749	1.641	1.858	2.074

[a] Z3 and Z5 denote 3T and 5T cluster models, respectively; O_B denotes the Brønsted oxygen; O_N denotes the neighboring bridging oxygen; H denotes the Brønsted proton [b] BSSE corrected binding energy.

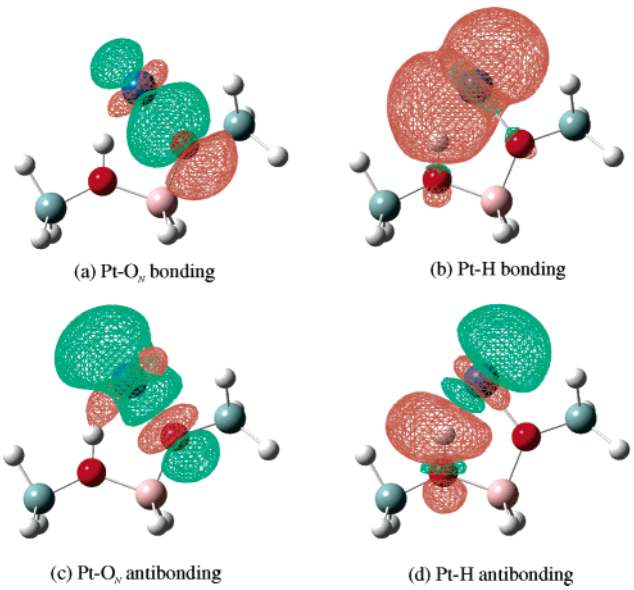

Figure 2. The natural bonding orbitals (NBO) plots of the Pt/H-ZSM-5 system.

TABLE 2: Partial Charges (au) and Electronic Configurations of Pt/H-ZSM-5

	partial charge (NAO)				electronic configuration	
systems	O_B	H	O_N	Pt	O_N	Pt
Pt(t)				0.00		6s(1.08)5d(8.92)
HZ3	−1.12	0.57	−1.27		2s(1.76)2p(5.50)	
PtHZ3	−1.18	0.43	−1.16	0.02	2s(1.75)2p(5.40)	6s(0.71)5d(9.27)
HZ5	−1.12	0.57	−1.29		2s(1.78)2p(5.49)	
PtHZ5	−1.19	0.41	−1.20	0.05	2s(1.76)2p(5.43)	6s(0.66)5d(9.27)

was linear in all systems. These illustrate that the Pt atom uses different orbtitals to bond with Brønsted proton and the C atom of CO. The Pt−C distances for all systems were about 1.8 Å. As seen from the lengthening of Pt−H (∼0.2 Å) and Pt−O_N distances (0.1 Å), interaction between the Pt atom and H-ZSM-5 was weakened significantly upon the adsorption of CO. Our calculated structural parameters of CO on Pt/H-ZSM-5 (in Table 3) agree very well with those from the EXAFS study of the adsorption of CO on Pt/LTL, providing a Pt−O distance of 2.28 ± 0.02 Å and a Pt−C distance of 1.92 ± 0.02 Å.[32] The small deviation of our results from the previous experimental results is probably due to differences in type and acidity of zeolites. The stretching mode of the Brønsted OH is shifted significantly from 1665 to 2795 cm^{-1}, corresponding to a shorter OH bond. The adsorption on the Pt atom can liberate the Brønsted proton and make the proton available for the consecutive catalyzed step.

The binding energy between CO and Pt-H-ZSM-5 (84.5 kcal/mol) was much larger than the binding energy between PtCO adduct and H-ZSM-5 (34.9 kcal/mol). The Pt−CO interaction is probably strong enough to cleave Pt atoms off of the Pt clusters, as is also suggested by CO-FTIR studies showing that neutral Pt/carbonyl complexes were formed in Pt/LTL zeolite[71] and that metal cluster size decreases upon adsorption of

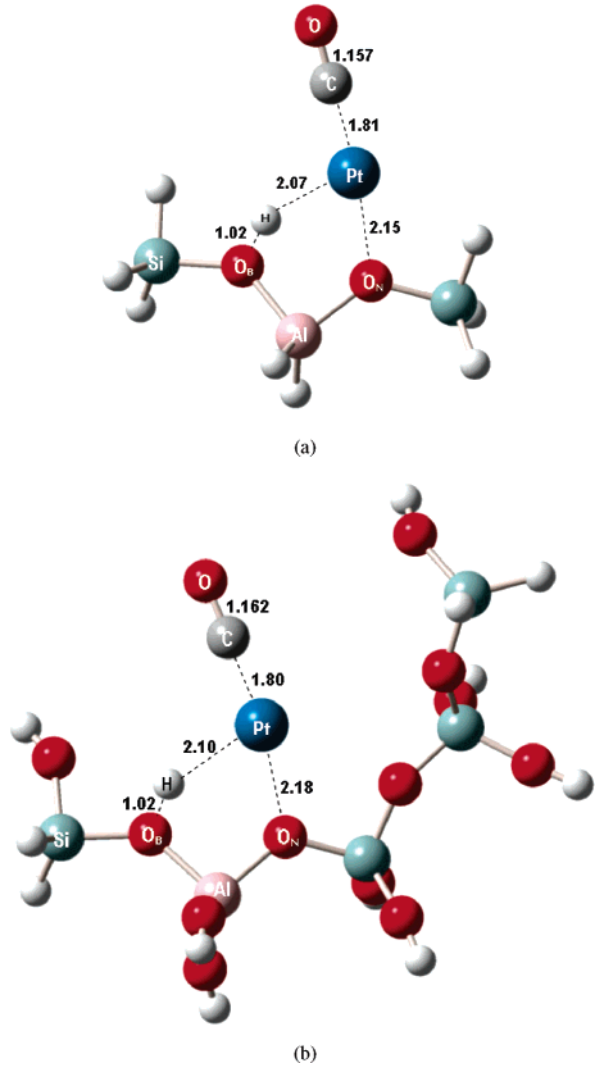

Figure 3. Optimized structures of CO adsorption on Pt/H-ZSM-5 (a) 3T and (b) 5T cluster models (selected bond distances are in Å).

CO.[27,32,38,71] The increased size of the zeolite model (from 3T to 5T) stabilized the adsorption of CO by 4.8 kcal/mol although it had little effect on the geometry. The difference between the binding energies predicted from 5T and 3T cluster models emphasizes the need of a realistic model to represent the zeolite framework since this can stabilize the adsorption complex.[71] Again, the changes in structural and energetic properties of CO adsorption on Pt/H-ZSM-5 due to the inclusion of Madelung potential were minor. The binding energy between CO and Pt/H-ZSM-5 was increased by only 0.5 kcal/mol. However, this is not true for all cases. For example, in the case of H_2 adsorption on Pt/H-ZSM-5, the Madelung potential had a more pronounced effect of decreasing the binding energy by as much as 5 kcal/mol.[67]

The interaction between CO and supported Pt can be examined by using NBO analysis. The bonding orbitals were formed between an occupied CO orbital and an unoccupied Pt−

TABLE 3: Selected Optimized Geometrical Parameters (Å) and Binding Energies E_B (kcal/mol) of Adsorptions of CO on Pt/Support

systems	E_B[a]	$R(AlO_B)$	$R(O_BH)$	$R(AlO_N)$	$R(Pt\cdots H)$	$R(Pt\cdots O_N)$	$R(Pt\cdots C)$	$R(CO)$[b]	$\Delta\nu(CO)$[c]
PtHZ3-CO	79.46	1.834	1.020	1.766	2.073	2.146	1.807	1.157	−20.7
PtHZ5-CO	84.24	1.806	1.023	1.733	2.096	2.179	1.794	1.162	−47.9 (−11.0)[d]
PtHZ10-CO	82.65[e]								−41.0 (−8.1)[d]

[a] BSSE correction included (4−8 kcal/mol). [b] Calculated isolated CO bond length = 1.138 Å. [c] Compared to experimentally isolated CO (2143 cm^{-1}). [d] Embedded cluster model. [e] Embedded 10T cluster calculation using the optimized 5T cluster structure.

TABLE 4: Partial Charges (au) and Electronic Configurations of Adsorptions of CO on Pt/Support

	partial charge (NAO)						electronic configuration	
systems	O_B	H	O_N	Pt	C	CO	O_N	Pt
HZ3-CO	−1.14	0.54	−1.14		0.51	0.06	2s(1.76)2p(5.50)	
PtHZ3-CO	−1.15	0.51	−1.25	−0.08	0.53	0.07	2s(1.75)2p(5.49)	6s(0.99)5d(9.09)
HZ5-CO	−1.14	0.54	−1.29		0.52	0.06	2s(1.78)2p(5.49)	
PtHZ5-CO	−1.16	0.51	−1.28	−0.04	0.51	0.01	2s(1.77)2p(5.50)	6s(0.97)5d(9.06)

O_N orbital and between occupied Pt d-orbitals and the unoccupied $2\pi^*$-orbital of CO (Figure 4). This interaction is comparable to the classical mechanism known as the π-back-bonding mechanism:[72] σ-donation from 5σ of CO to sd-hybrid orbitals of Pt and π-back-donation from d-orbitals of Pt to $2\pi^*$ of CO. The π-back-donation weakens the CO bond because of the antibonding nature of $2\pi^*$ orbitals. Although the net charge of the CO molecule was slightly positive, the latter process (bonding between occupied Pt d-orbitals and the unoccupied $2\pi^*$-orbital of CO or the analogous π-back-donation) is very important, as can be seen from the significant increase of electron density in π^*-orbtials of CO and the lengthening of the CO bond. The CO bond was lengthened by as much as 0.025 Å when adsorbed on Pt-HZSM-5, corresponding to the red-shifted stretching frequency.

As mentioned earlier, the frequency shift of adsorbed CO has been used to determine the electronic state of Pt clusters and to validate the computational models. An experiment has reported that the band at 2123 cm^{-1} assigned to CO adsorption on monatomic Pt is very stable and still remains in the spectra even after desorption at 623 K.[37] The stretching frequency of adsorbed CO calculated from the bare 5T cluster model was 2095.1 cm^{-1}. This 49 cm^{-1} red shift is somewhat larger than the observed 20 cm^{-1} red shift from experiment. Although the stretching mode of 2123 cm^{-1} determined from the 3T cluster matches perfectly with the experimental finding, it can be considered the result of fortunate error-cancellation for this model. Our previous study of CO adsorptions on Cu-ZSM-5[55] showed that the stretching mode of CO is very sensitive to its environment, especially to the Madelung potential from the zeolite framework. Inclusion of the Madelung potential by using the SCREEP embedding scheme brought ν_{CO} to 2132.0 cm^{-1} (11 cm^{-1} red shift), agreeing with the experimental finding. This emphasizes the importance of the long-range effect of the framework on the vibrational modes of the adsorbates.

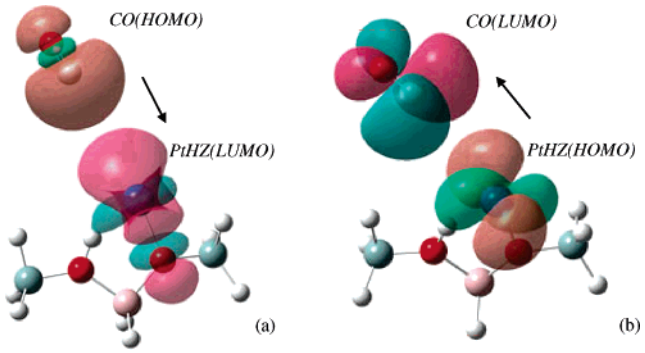

Figure 4. The interaction between the Pt/H-ZSM-5 and a CO molecule can be explained by the π-back-bonding processes: (a) σ donation and (b) π-back-donation. The arrows show the directions of electron transfer.

The effects of the cluster size were investigated by performing both cluster and embedded cluster calculations with the 10T cluster as shown in Figure 1c. In these calculations, the optimized 5T structures were used while the remaining quantum atoms of the 10T cluster were fixed in their experimental lattice positions. The binding energy of CO to Pt/H-ZSM-5 with this model was decreased by only 1.6 kcal compared to that of the embedded 5T model (see Table 3). Despite the large differences between the results from the CO adsorptions on 3T and 5T clusters, we found that frequencies of adsorbed CO calculated from the embedded 5T and 10T clusters are only 2.9 cm^{-1} different. These results confirm that the embedded 5T cluster would provide a cost-effective model for studying adsorption of small molecules in the Pt/H-ZSM-5 system. The same conclusion had been made in our previous study of CO adsorption on Cu-ZSM-5.[55]

The H-ZSM-5 support not only withdraws electron density from the Pt atom to the acidic proton, but it also provides electron density to the Pt atom through the framework oxygen. Thus the electron transfer from Pt atom to the proton seems not to have a considerable effect on the π-back-donation and the electron deficient state may not be the key reason for the notably small red shift. We suggest that the change in electronic properties of Pt is due to its interaction with the acid site and the Madelung potential from the zeolite framework. The shift of CO may not directly reflect the local properties of a Pt atom in H-ZSM-5 because the Madelung potential also has an influence on the stretching frequency of CO.

4. Conclusion

The interaction between platinum atom and H-ZSM-5 has been examined by using the DFT/B3LYP level of calculation with mixed basis sets. The choice of models representing the active site of the zeolite is critical to explain the interaction between Pt and H-ZSM-5 correctly. We found that a Pt atom interacts with a Brønsted proton and with a nearby bridging framework oxygen. The binding energy of Pt on the Brønsted acid is 15 kcal/mol. The electron transfer between Pt atom and H-ZSM-s results in an electron redistribution in the Pt atom, with more electron density in the s-orbital and less in the

d-orbital. A shift of Pt's d-orbitals due to interaction with the zeolite surface was observed. These results suggest that without the Brønsted acid site the Pt atom is not stable in H-ZSM-5 and so agglomeration of Pt atoms to form a larger particle is expected. The effect of the H-ZSM-5 support is not only to withdraw electron density from the Pt atom to the acidic proton, but also to provide electron density to the Pt atom through the framework oxygen.

The adsorption of carbon monoxide was also investigated. With use of the embedded cluster model, our model predicted an 8−11 cm^{-1} red shift of adsorbed CO on Pt/H-ZSM-5, matching well with the experimental 20 cm^{-1} red shift. The frequency shift of adsorbed CO on the zeolite surface reflects not only the electronic structure of supported Pt but also the extended zeolite framework environment. The Madelung potential was found to be necessary to obtain the accurate vibrational frequency and binding energy. The π-back-donation between CO and Pt/H-ZSM-5 was significant, as is seen from the increase of electron density in π^*-orbtials of CO.

Acknowledgment. This work was supported in part by the Thailand Research Fund (TRF), the University of Utah, and the National Science Foundation. Computer support from the Center for High Performance Computing at the University of Utah is gratefully acknowledged

References and Notes

(1) Bandiera, J.; Naccache, C.; Imelik, B. *J. Chim. Phys. Phys.-Chim. Biol.* **1978**, *75*, 406.
(2) Chupin, J.; Gnep, N. S.; Lacombe, S.; Guisnet, M. *Appl. Catal., A* **2001**, *206*, 43.
(3) Blomsma, E.; Martens, J. A.; Jacobs, P. A. *Stud. Surf. Sci. Catal. B* **1997**, *105*, 909.
(4) Watanabe, M.; Uchida, H.; Igarashi, H.; Suzuki, M. *Chem. Lett.* **1995**, 21.
(5) Iwamoto, M.; Hernandez, A. M.; Zengyo, T. *Chem. Commun.* (*Cambridge*) **1997**, 37.
(6) Benvenutti, E. V.; Franken, L.; Moro, C. C.; Davanzo, C. U. *Langmuir* **1999**, *15*, 8140.
(7) Davis, R. J. *Heterog. Chem. Rev.* **1994**, *1*, 41.
(8) Dong, J.-L.; Zhu, J.-H.; Xu, Q.-H. *Appl. Catal., A* **1994**, *112*, 105.
(9) Cho, B. K.; Yie, J. E. *Appl. Catal., B* **1996**, *10*, 263.
(10) Gallezot, P. *Mol. Sieves* **2002**, *3*, 257.
(11) Samant, M. G.; Boudart, M. *J. Phys. Chem.* **1991**, *95*, 4070.
(12) Sachtler, W. M. H. *Acc. Chem. Res.* **1993**, *26*, 383.
(13) Stakheev, A. Y.; Kustov, L. M. *Appl. Catal., A* **1999**, *188*, 3.
(14) Zhidomirov, G. M.; Yakovlev, A. L.; Milov, M. A.; et al. *Catal. Today* **1999**, *51*, 397.
(15) Bandiera, J. *J. Chim. Phys. Phys.-Chim. Biol.* **1980**, *77*, 303.
(16) Silva, J. M.; Ribeiro, M. F.; Ramoa Ribeiro, F.; et al. *Appl. Catal., A* **1995**, *125*, 1.
(17) Galperin, L. B.; Bricker, J. C.; Holmgren, J. R. *Appl. Catal., A* **2003**, *239*, 297.
(18) Sugioka, M.; Tochiyama, C.; Matsumoto, Y.; Sado, F. *Stud. Surf. Sci. Catal.* **1995**, *94*, 544.
(19) Kurosaka, T.; Sugioka, M.; Matsuhashi, H. *Bull. Chem. Soc. Jpn.* **2001**, *74*, 757.
(20) Vasina, T. V.; Masloboishchikova, O. V.; Khelkovskaya-Sergeeva, E. G.; et al. *Stud. Surf. Sci. Catal.* **2001**, *135*, 4207.
(21) Arribas, M. A.; Martinez, A. *Appl. Catal., A* **2002**, *230*, 203.
(22) Noordhoek, N. J.; Schuring, D.; de Gauw, F. J. M. M.; et al. *Ind. Eng. Chem. Res.* **2002**, *41*, 1973.
(23) Kuznetsov, P. N. *J. Catal.* **2003**, *218*, 12.
(24) Mills, G. A.; Heinemann, H.; Milliken, T. H.; Oblad, A. G. *Ind. Eng. Chem.* **1953**, *45*, 134.
(25) Weisz, P. B.; Swegler, E. W. *Science* **1957**, *126*, 31.
(26) Kuhlmann, A.; Roessner, F.; Schwieger, W.; et al. *Catal. Today* **2004**, *97*, 303.
(27) Mojet, B. L.; Miller, J. T.; Ramaker, D. E.; Koningsberger, D. C. *J. Catal.* **1999**, *186*, 373.
(28) Gallezot, P.; Alarcon-Diaz, A.; Dalmon, J. A.; et al. *J. Catal.* **1975**, *39*, 334.
(29) Lane, G. S.; Miller, J. T.; Modica, F. S.; Barr, M. K. *J. Catal.* **1993**, *141*, 465.
(30) Sharma, S. B.; Miller, J. T.; Dumesic, J. A. *J. Catal.* **1994**, *148*, 198.
(31) Vaarkamp, M.; Miller, J. T.; Modica, F. S.; et al. *Stud. Surf. Sci. Catal.* **1993**, *75*, 809.
(32) Mojet, B. L.; Miller, J. T.; Koningsberger, D. C. *J. Phys. Chem., B* **1999**, *103*, 2724.
(33) Khodakov, A.; Barbouth, N.; Berthier, Y.; et al. *J. Chem. Soc., Faraday Trans.* **1995**, *91*, 569.
(34) Boyanov, B. I.; Morrison, T. I. *J. Phys. Chem.* **1996**, *100*, 16318.
(35) Cho, S. J.; Ahn, W.-S.; Hong, S. B.; Ryoo, R. *J. Phys. Chem.* **1996**, *100*, 4996.
(36) Lerner, B. A.; Carvill, B. T.; Sachtler, W. M. H. *J. Mol. Catal.* **1992**, *77*, 99.
(37) Stakheev, A. Y.; Shpiro, E. S.; Tkachenko, O. P.; et al. *J. Catal.* **1997**, *169*, 382.
(38) Zholobenko, V. L.; Lei, G. D.; Carvill, B. T.; et al. *J. Chem. Soc., Faraday Trans.* **1994**, *90*, 233.
(39) Tzou, M. S.; Sachtler, W. M. H. *Stud. Surf. Sci. Catal.* **1988**, *38*, 233.
(40) Dalla Betta, R. A.; Boudart, M. *Catal., Proc. Int. Congr., 5th* **1973**, *2*, 1329.
(41) Datka, J.; Gallezot, P.; Massardier, J.; Imelik, B. *Rev. Port. Quim.* **1977**, *19*, 297.
(42) Weber, R. S.; Boudart, M.; Gallezot, P. *Stud. Surf. Sci. Catal.* **1980**, *4*, 415.
(43) Miller, J. T.; Mojet, B. L.; Ramaker, D. E.; Koningsberger, D. C. *Catal. Today* **2000**, *62*, 101.
(44) Vedrine, J. C.; Dufaux, M.; Naccache, C.; Imelik, B. *Proc. Int. Vac. Congr., 7th* **1977**, *1*, 481.
(45) Sachtler, W. M. H.; Zhang, Z. *Adv. Catal.* **1993**, *39*, 129.
(46) Gruenert, W.; Muhler, M.; Schroeder, K.-P.; et al. *J. Phys. Chem.* **1994**, *98*, 10920.
(47) Mojet, B. L.; Kappers, M. J.; Miller, J. T.; Koningsberger, D. C. *Stud. Surf. Sci. Catal.* **1996**, *101*, 1165.
(48) Hammer, B.; Norskov, J. K. *Nature* (*London*) **1995**, *376*, 238.
(49) Grillo, M. E.; Ramirez de Agudelo, M. M. *J. Mol. Model.* **1996**, *2*, 183.
(50) Yakovlev, A. L.; Neyman, K. M.; Zhidomirov, G. M.; Roesch, N. *J. Phys. Chem.* **1996**, *100*, 3482.
(51) Grillo, M. E.; Ramirez de Agudelo, M. M. *J. Mol. Catal., A* **1997**, *119*, 105.
(52) Watwe, R. M.; Spiewak, B. E.; Cortright, R. D.; Dumesic, J. A. *Catal. Lett.* **1998**, *51*, 139.
(53) Curulla, D.; Clotet, A.; Ricart, J. M.; Illas, F. *J. Phys. Chem., B* **1999**, *103*, 5246.
(54) Ramaker, D. E.; de Graaf, J.; van Veen, J. A. R.; Koningsberger, D. C. *J. Catal.* **2001**, *203*, 7.
(55) Treesukol, P.; Limtrakul, J.; Truong, T. N. *J. Phys. Chem. B* **2001**, *105*, 2421.
(56) Derouane, E. G.; Fripiat, J. G. *Zeolites* **1985**, *5*, 165.
(57) Alvarado-Swaisgood, A. E.; Barr, M. K.; Hay, P. J.; Redondo, A. *J. Phys. Chem.* **1991**, *95*, 10031.
(58) Schroeder, K. P.; Sauer, J.; Leslie, M.; Catlow, C. R. A. *Zeolites* **1992**, *12*, 20.
(59) Stefanovich, E. V.; Truong, T. N. *J. Phys. Chem. B* **1998**, *102*, 3018.
(60) Vollmer, J. M.; Stefanovich, E. V.; Truong, T. N. *J. Phys. Chem. B* **1999**, *103*, 9415.
(61) Limtrakul, J.; Khongpracha, P.; Jungsuttiwong, S.; Truong, T. N. *J. Mol. Catal. A*: *Chem.* **2000**, *153*, 155.
(62) Hay, P. J.; Wadt, W. R. *J. Chem. Phys.* **1985**, *82*, 299.
(63) Boys, S. F.; Bernadi, F. *Mol. Phys.* **1970**, *19*, 553.
(64) Simon, S.; Duran, M.; Dannenberg, J. J. *J. Chem. Phys.* **1996**, *105*, 11024.
(65) Reed, A. E.; Weinhold, F.; Curtiss, L. A.; Pochatko, D. J. *J. Chem. Phys.* **1986**, *84*, 5687.
(66) Frisch, M. J.; Trucks, G. W.; Schlegel, H. B.; et al. *Gaussian03*, Revision A.1; Gaussian, Inc: Pittsburgh, PA, 2003.
(67) Treesukol, P.; Truong, T. N. Unpublished results.
(68) Gallezot, P.; Bergeret, G. *Stud. Surf. Sci. Catal.* **1982**, *12*, 167.
(69) Sachtler, W. M. H.; Tzou, M. S.; Jiang, H. J. *Solid State Ionics* **1988**, *26*, 71.
(70) Kampers, F. W. H.; Engelen, C. W. R.; Van Hooff, J. H. C.; Koningsberger, D. C. *J. Phys. Chem.* **1990**, *94*, 8574.
(71) Stakheev, A. Y.; Shpiro, E. S.; Jaeger, N. I.; Schulz-Ekloff, G. *Catal. Lett.* **1995**, *34*, 293.
(72) Blyholder, G. *J. Phys. Chem.* **1964**, *68*, 2772.